


## Article

# Life Analysis of Reusable Liquid Rocket Engine Thrust Chamber

Yuanjie Qi <sup>1</sup>, Yuqiang Cheng <sup>2</sup> and Yan Zhang <sup>1,\*</sup> <sup>1</sup> School of Aeronautics and Astronautics, Sun Yat-sen University, Shenzhen 518000, China<sup>2</sup> College of Aerospace Science and Engineering, National University of Defense Technology, Changsha 410073, China

\* Correspondence: zhangyan25@mail.sysu.edu.cn

**Abstract:** The thrust chamber's inner wall suffers high temperature and pressure differences from the coolant channel, which limits the life of the rocket engine. Life prediction of the thrust chamber really plays an important role in reusable launch vehicle propulsion systems. The Porowski beam model is widely used in the life prediction of reusable liquid rocket engine thrust chambers, which calculates the life caused by fatigue, creep, and thinning after each firing cycle. In order to analyze the life of the thrust chamber, a LOX/Kerosene rocket engine is investigated in this paper. The life analysis consists of pressure and temperature differences and structural parameters. Two kinds of inner wall materials were chosen for comparison in this research: OFHC copper and Narloy-Z alloy. The results are presented to offer a reference for the design and manufacture of reusable rocket engine thrust chambers in the future.

**Keywords:** life; reusable liquid rocket engine; thrust chamber; Porowski beam model; inner wall; ligament



**Citation:** Qi, Y.; Cheng, Y.; Zhang, Y. Life Analysis of Reusable Liquid Rocket Engine Thrust Chamber. *Aerospace* **2022**, *9*, 788. <https://doi.org/10.3390/aerospace9120788>

Academic Editor: Justin Hardi

Received: 9 October 2022

Accepted: 24 November 2022

Published: 2 December 2022

**Publisher's Note:** MDPI stays neutral with regard to jurisdictional claims in published maps and institutional affiliations.



**Copyright:** © 2022 by the authors. Licensee MDPI, Basel, Switzerland. This article is an open access article distributed under the terms and conditions of the Creative Commons Attribution (CC BY) license (<https://creativecommons.org/licenses/by/4.0/>).

## 1. Introduction

Liquid rocket engine suffers high temperature and pressure difference which is the reason for failure and life limitation, shown in Figure 1. With the rapid development of reusable technology for liquid rocket engines (LREs), life prediction of the key component has to be considered after each launching procedure. There are many life prediction methods for liquid rocket engine thrust chambers, such as stress-strain methods, beam models, unified visco-plastic models, and finite element analyses.

H. J. Kasper [1] developed an analytical method that modeled the cyclic creep failure phenomenon for the Space Shuttle Main Engine (SSME). The research provided advice for increasing the life of thrust chambers. A.K. Asraff [2,3] performed a stress analysis and cyclic and creep life prediction of a cryogenic rocket engine thrust chamber materials by ANSYS finite element analysis software package. The failure mode of stainless steel and copper alloys are creep and low cycle fatigue (LCF). The research also explored the different alloy plasticity models and details of cyclic stress analysis carried out for the double-walled rocket engine thrust chamber. W. Schwarz [4] developed a model that quantitatively accounted for the crack failure mechanism of the thrust chamber's hot-gas-side wall and verified it using 3D finite element simulation data. Tong Jun [5] aimed at the problem of the muster and ablation on the inner wall of the thrust chamber throat section, a three-dimensional analysis of modeling finite element was conducted to calculate the steady creep and accelerated creep deformation of the structure in the high-temperature phase. Cheng Cheng [6] investigated the thermo-mechanical response of channel wall nozzles under cyclic working loads, and the finite volume fluid-thermal coupling calculation method and the finite element thermal-structural coupling analysis technique are applied. A simplified nonlinear damage accumulation approach has been suggested to estimate the fatigue service life of the channel wall nozzle, which is obviously conservative to the Miner's life. Zhang sheng [7] established a structural model based on finite elements to evaluate the cooling channel of thrust chamber reliability. The parameter sensitivity was analyzed and demonstrated the dangerous point of the thrust chamber's inner wall.

M. Ferraiuolo [8,9] performed numerical investigations on the influence of the closeout geometry and materials on the number of cycles to failure of the thrust chamber. The impact of the creep phenomenon on the service life was also illustrated by Viscoplastic models. M. Ferraiuolo [10] also researched a global linear model and a local nonlinear model to improve the accuracy of the numerical simulations. Citarella R. [11] investigated the main failure phenomena that could occur during the thrust chamber's service life using non-linear finite element analyses. The most critical areas appeared on the inner surface of the chamber, which was consistent with experimental tests from literature conducted on similar geometries. Di Liu [12] developed a Finite Element Method (FEM) based on experimental data in order to evaluate the structural failure risk of the regenerative cooling thrust chamber inner wall. The multi-cycle thermo-structural analysis demonstrated the evolution of the stress-strain curve and damage analysis for dangerous points.

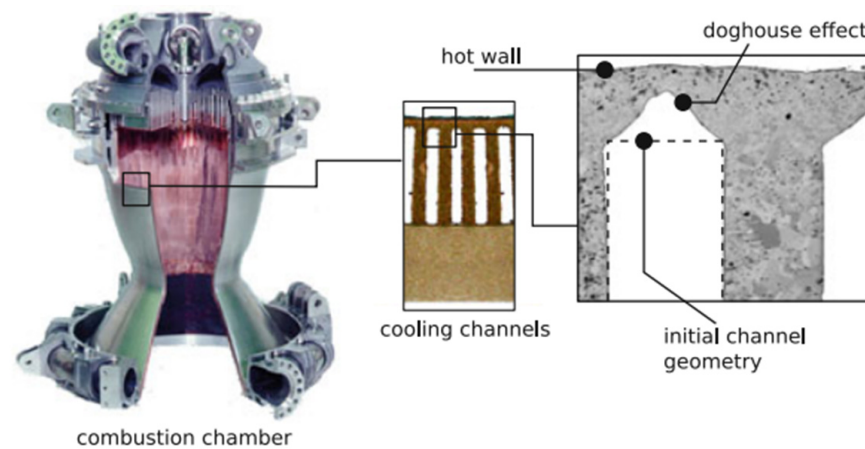


**Figure 1.** Dog-house failure of thrust chamber inner wall [4].

However, except for the beam model, most of the life prediction methods are quite difficult to conduct life analyses for because of complex mathematical expressions and fail to demonstrate the thinning of the inner wall [13]. The beam model is a simplified method to reveal the life of reusable liquid rocket engines, which contains the Porowski clamped beam model, the creep-modified model, and the sandwich beam model [14,15].

The Porowski beam model is a simplified model for the thrust chamber inner walls, which considers the ligament as a clamped beam. This model was first proposed by J.S. Porowski and M. Badlani for the Space Shuttle Main Engine (SSME) and is still widely used in thrust chamber life prediction because of its convenience until now. Porowski [16,17] developed the clamped beam model to predict the life of the SSME main combustion chamber, which first offers the deformation and strain range of the coolant channel on the side of the gas wall and takes into account the plastic ratchet effect. The calculation results are verified through finite element analysis, and the results are relatively satisfactory. Badlani [18] improved the previous clamped beam life model, increased the deformation caused by creep, and considered the impact of fatigue and ratchet damage in the life prediction. Combining the relevant parameters of SSME to calculate thinning of the coolant channel liner under one cycle, it's almost consistent with the results of the finite element analysis, which verifies the effectiveness and accuracy of this method. The creep-modified beam model can estimate the life of the inner wall after a working cycle, and the life calculation results are more conservative than other methods.

M. Niino [19], in order to improve the performance of high-pressure thrust chamber closeout and increase the life of the thrust chamber, developed the cold isostatic pressing (CIP) forming method. The Porowski beam model was used to predict the life of the thrust chamber, and the lifetime was 37 cycles for case A and 390 cycles for case B, respectively. The firing test was performed to verify the results. In-Kyung Sung [20] analyzed the life of the SSME inner wall and calculated the temperature field, plastic strain and deformation by the

Porowski beam model and other methods. The estimated life of the Porowski beam model is 67 cycles. Tao Chen [21] used the creep-modified Porowski beam model to estimate the life of a reusable liquid engine thrust chamber in the throat section. The life prediction results offered a reference for the design of reusable thrust chambers. Marco Pizzarelli [22,23] developed an algebraic model for structural and life analysis of regeneratively cooled thrust chambers. The life of instability is calculated by the Porowski beam model. The calculation results are verified by experimental data from NASA Lewis Research Center.

Although the Porowski beam model is widely used in thrust chamber life prediction, life analysis of this model is infrequent in many articles. Life analysis is critical in reusable thrust chamber design and manufacture. The present work aims at the life analysis of LRE thrust chambers using the Porowski beam model by derivation and simulation.

### 2. Basic Equations and Procedures of the Porowski Beam Model

In the Porowski beam model, the ligament of the inner wall is considered a clamped beam, in which both ends are constrained. The inner wall of the thrust chamber suffers from high temperature and pressure differences between the hot-gas-side wall and coolant channel wall, which causes incremental damage and thinning after each working cycle. The simplified structure of the thrust chamber is shown in Figure 2.

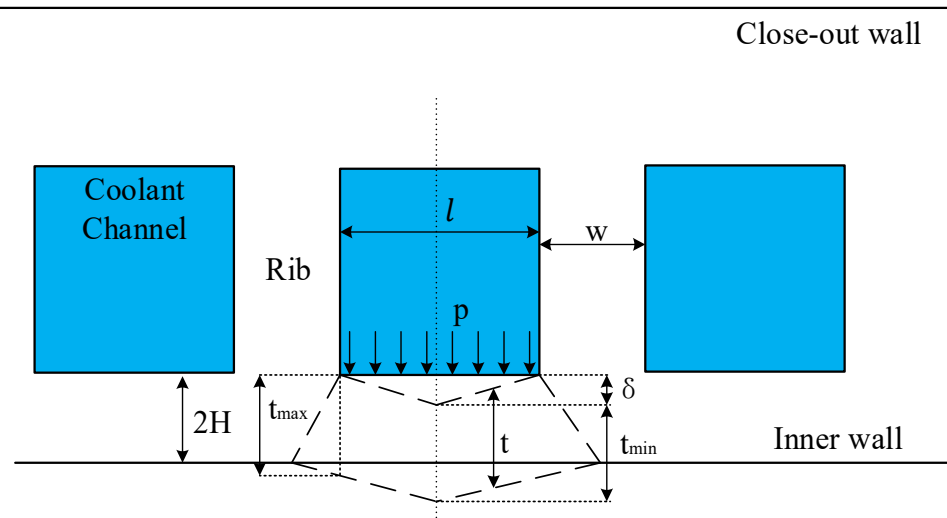


Figure 2. Simplified structure of thrust chamber inner wall.

#### 2.1. Inelastic Strain

The average temperatures of the inner wall ligament and closeout wall were denoted by  $T_i$  and  $T_0$ , respectively. The inelastic strain range of the Porowski model and creep-modified model are given by Equations (1) and (2).  $T_i$  and  $T_0$  can be calculated from Equations (3) and (4). The coefficient of  $\bar{A}$  is taken as 0.35 for the rectangular coolant channel in Equation (4).

$$\Delta \epsilon'_{pl} = \alpha [(T_i - T_0)_{max} - (T_i - T_0)_{min}] - \frac{2S_y}{E} \tag{1}$$

$$\Delta \epsilon'_{pl} = \left\{ \alpha [(T_i - T_0)_{max} - (T_i - T_0)_{min}] - \frac{2S_y}{E} \right\} + \frac{\Delta \sigma_c}{E} \tag{2}$$

$$T_i = \frac{T_{wg} + T_{wc}}{2} \tag{3}$$

$$T_0 = \bar{A} T_i \tag{4}$$

During the ignition and steady-state working conditions, there is also a temperature drop across the ligament, which causes bending, because the inner wall ends are clamped. Conservatively assuming that all of the available elastic energy goes into plastic straining of the ligament, the correction due to thermally induced bending is given by:

$$\Delta \varepsilon''_{pl} = \frac{E(\alpha \Delta T)^2}{12(1 - \mu)^2 S_y} \quad (5)$$

Then, the total inelastic strain for the complete cycle is:

$$\varepsilon_1 = 2(\Delta \varepsilon'_{pl} + \Delta \varepsilon''_{pl}) \quad (6)$$

The coefficient of thermal expansion is  $\alpha$ ,  $S_y$  is the yield stress,  $\Delta \sigma_c = S_y$  is the creep relaxation stress,  $E$  for Young's modulus,  $\mu$  for Poisson's ratio.  $T_{wg}$  and  $T_{wc}$  are hot-gas-side wall temperature and coolant channel wall temperature, which can be obtained by heat transfer analysis, and  $\Delta T$  is temperature drop across the inner wall ligament.

### 2.2. Deflection

Bending deflection  $\delta_1$ , shear deflection  $\delta_2$  and creep-induced deflection  $\delta_3$  of the ligament are given by Equations (7) and (9) as follows.

The pressure difference between the coolant channel and thrust chamber is  $p$ , and  $l$  is the length of the coolant channel.  $B$  and  $r$  are the material constants,  $t$  is the firing time,  $2H$  is the thickness of the ligament and  $\bar{F}(r)$  has been tabulated for various  $r$ -values in reference [18].

The total deflection per cycle of the Porowski beam model and creep-modified model are  $\delta = \delta_1 + \delta_2$  and  $\delta = \delta_1 + \delta_2 + \delta_3$ , respectively. This is accomplished with the assumption that the deflection during each firing cycle remains constant.

$$\delta_1 = 2 \left( \frac{H}{\varepsilon_1} - \sqrt{\left( \frac{H}{\varepsilon_1} \right)^2 - \left( \frac{l}{4} \right)^2} \right) \quad (7)$$

$$\delta_2 = \frac{\varepsilon_1 p l^2}{4HS_y} \quad (8)$$

$$\delta_3 = \frac{Bt l^2}{4H} \left( \frac{p l^2}{16H^2} \right)^r \bar{F}(r) \quad (9)$$

### 2.3. Ligament Deformation

Experimental evidence from NASA Lewis Research Center [24,25] shows that the distorted shape of the inner wall can be approximated by a linear variation in thickness thinning. Thus using the linear thinning model developed in the Porowski model, the thinning after  $N$  cycles,  $t_N$ , is then given by:

$$t_N = \frac{Nw\delta}{l + w} \quad (10)$$

Based on the linear variation assumption, the thickness of the inner wall ligament can be described by  $t_{min}$  and  $t_{max}$  after  $N$  cycles which are given by Equations (11) and (12). The symbol  $t_{max}$  means the thickness of the end of the inner wall ligament, which increases during the firing cycle, and the symbol  $t_{min}$  means the thickness of the middle section of the inner wall ligament, which decreases during the firing cycle.

$$t_{\min} = \frac{2H(l+w) - Nw\delta}{l+w} \quad (11)$$

$$t_{\max} = \frac{2H(l+w)^2 + Nw\delta}{(l+w)^2} \quad (12)$$

#### 2.4. Fatigue and Creep Rupture Damage

According to the linear thinning model of the inner wall, the effective strain range in the section of minimum ligament for entering the fatigue curve is then:

$$\varepsilon_t = \frac{2}{\sqrt{3}} \sqrt{\varepsilon_{1\min}^2 + \varepsilon_{1\min}\varepsilon_{2\min} + \varepsilon_{2\min}^2} \quad (13)$$

The hoop strain of the inner wall ligament in the minimum section is calculated by:

$$\varepsilon_{1\min} = \varepsilon_{1\text{avg}} \frac{q-1}{q} \left( \frac{t_{\max}}{t_{\min}} - 1 \right) \left[ \left( \frac{t_{\max}}{t_{\min}} \right)^{\frac{q-1}{q}} - 1 \right]^{-1} \quad (14)$$

$$q = 0.2 \left( \frac{S_u - S_y}{S_y} \right)^{0.6} \quad (15)$$

The ultimate strength of inner wall material is  $S_u$ , and  $\varepsilon_t$  is the effective strain range.

The average hoop strain  $\varepsilon_{1\text{avg}}$  and the axial strain  $\varepsilon_{2\min}$  in the minimum ligament section are given by:

$$\varepsilon_{1\text{avg}} = \alpha(T_i - T_0) \quad (16)$$

$$\varepsilon_{2\min} = \alpha(T_i - T_0) \quad (17)$$

#### 2.5. Life Prediction

The life of the thrust chamber contains plastic instability life and fatigue-creep life according to the Porowski model based on different failure modes. Life of instability is given by the following Equation (18) and  $q$  is the ratio of  $S_u$  and  $S_y$ . The critical thickness at the life of instability is given by (18):

$$2H(1 - e^{-q}) = t_{\text{cr}}, t_N = t_{\text{cr}} \quad (18)$$

For some inner wall materials, the number of cycles at which ligament thinning stops  $N_T$  is related to the strain hardening parameter  $q$ . The following empirical criterion is obtained from reference [17]:

$$N_T = 750q^{1.25} \quad (19)$$

Fatigue curve of thrust chamber inner wall material matched by Manson Universal Slopes (MUS) Equation.

$$\varepsilon_t = 3.5 \left( \frac{S_u}{E} \right) N_F^{-0.12} + \varepsilon_f^{0.6} N_F^{-0.6} \quad (20)$$

$$\varepsilon_f = \ln \left( \frac{100}{100 - \%RA} \right) \quad (21)$$

The fatigue life of this material is  $N_F$ , %RA stands for the reduction in area.  $S_u$  and  $S_y$  for both materials are shown in Section 3.2. The stress-to-rupture curves of OFHC copper and Narloy-Z using data matched using the MUS equation are shown in Figure 3.

Therefore, the procedure of life prediction of the thrust chamber is shown in Figure 4. Firstly, the parameters of the combustion chamber should be acquired.

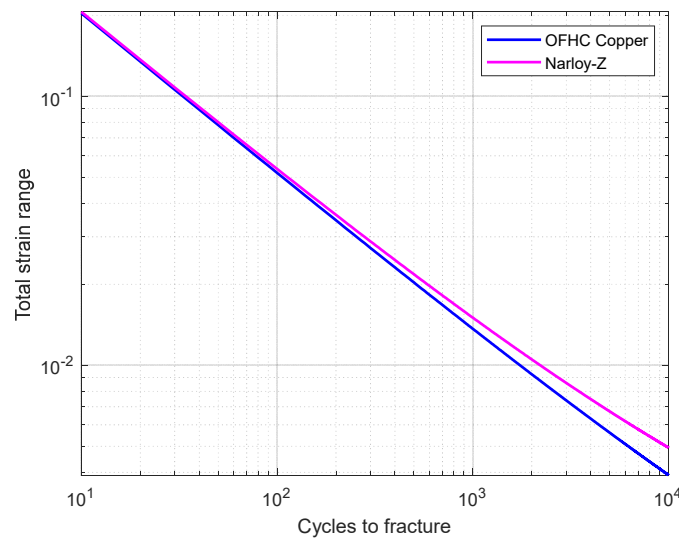


Figure 3. Fatigue curve of OFHC copper and Narloy-Z matched by MUS equations.

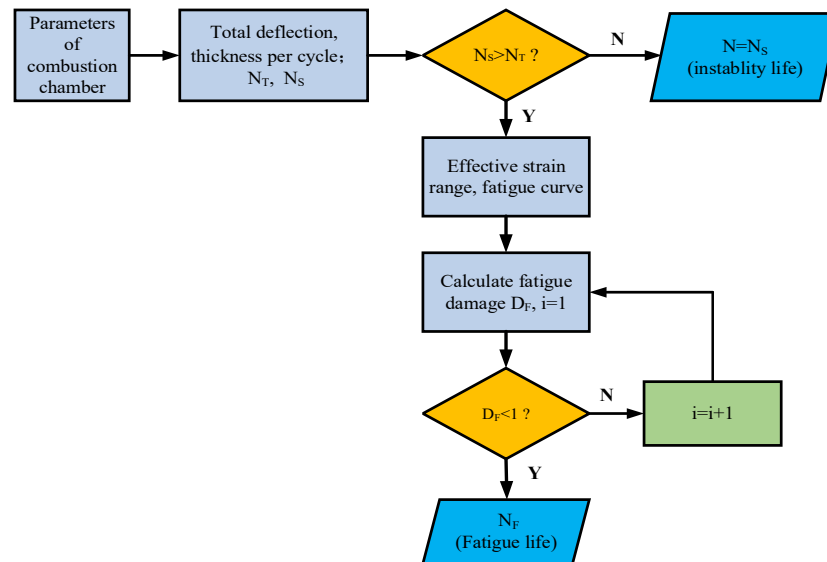


Figure 4. Life prediction procedure of the Porowski beam model.

### 3. Parameters Input

In the Porowski beam model, the parameter of the liquid rocket engine and inner wall materials of the thrust chamber should be given before life prediction.

#### 3.1. Thrust Chamber Parameters

In this article, a LOX/Kerosene rocket engine is taken as an object of investigation. The main features of the LOX/Kerosene rocket engine, which are input in RPA (rocket propulsion analysis), are given in Table 1. Thermal analysis of this type of thrust chamber is shown in Figure 5.

Table 1. Main features of LOX/Kerosene rocket engine.

Parameters	Value	Unit
chamber pressure	18.0	MPa
chamber length	2291	mm
components mass ratio	2.6 <sup>1</sup>	/
expansion area ratio	35	/

<sup>1</sup> means the ratio of oxygen and kerosene.

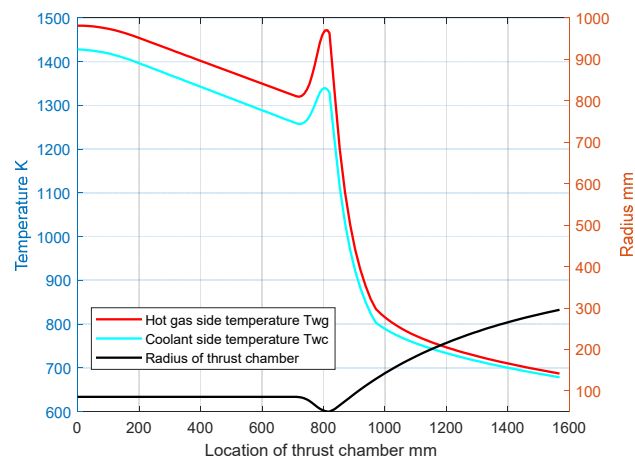


**Figure 5.** Temperature of the gas-side wall and coolant-side wall.

The chamber pressure of the LOX/Kerosene rocket engine is 18.0 MPa (2610.68 psi) of steady state during the firing cycle. From thermal analysis by RPA software simulation,  $T_{wg}$  for gas-side wall temperature is 1472.03 K and  $T_{wc}$  for coolant channel wall temperature is 1336.62 K, the temperature drop across the ligament in the throat section is 135.41 K (243.73 °F).

The parameters put into the Porowski beam model are given in Table 2.

**Table 2.** Parameters of the thrust chamber.

Parameters	Value	Unit
firing time $t$	4	min
width of the coolant channel $l$	1.686	mm
width of rib $w$	1.270	mm
thickness of ligament $2H$	0.889	mm

### 3.2. Material Parameters

Two kinds of widely used inner wall materials are chosen for the thrust chamber ligament, OFHC copper and Narloy-Z alloy. Parameters of those two kinds of inner wall materials are given in Table 3. OFHC copper is an oxygen-free grade of essentially pure copper, which is widely used in cryogenic rocket engine thrust chambers. Narloy-Z alloy is a copper base alloy containing a nominal three percent silver and 0.5 percent zirconium. The silver-zirconium-copper alloy combines high electrical and thermal conductivity with moderate strength retention at high temperatures [26,27].

**Table 3.** Parameters of inner wall material.

Material	$\mu$	E (MPa)	$S_u$ (MPa)	$S_y$ (MPa)
OFHC	0.3	117215	317	62
Narloy-Z	0.34	124110	379	207

## 4. Life Analysis

The life analysis of the thrust chamber contains pressure difference and temperature differences between the inner wall, structural parameters and material parameters. Except for pressure difference analysis, the rest of the chamber pressure difference is set at 18.0 MPa.

The failure of this LOX/Kerosene rocket engine is plastic instability, according to Figure 4, so the deflection per cycle and the life of instability are analyzed.

The figure legend with (P) is the result of the Porowski beam model, and the figure legend with (C) stands for the creep-modified model. Two kinds of inner wall materials, OFHC and Narloy-Z, are analyzed as a comparison. The deflections of both materials calculated by the model are given in Table 4.

**Table 4.** Deflection of inner wall material.

Material	Porowski Model	Creep Modified Model	Unit
OFHC	0.02321636	0.02413356	mm
Narloy-Z	0.01076731	0.01364412	mm

**4.1. Pressure Difference**

The pressure difference range of this LOX/Kerosene liquid rocket engine thrust chamber set in this research is 10–30 MPa because of its full-flow staged combustion cycle. The relationship between pressure difference, deflection per cycle and life of instability are shown in the pictures as follows. It can be seen from Figures 6 and 7 that the deflection and life of instability under the Porowski beam model approximately obey a linear relationship. The deflection of OFHC copper is higher than the Narloy-Z alloy. However, the life of instability seems different, and OFHC copper seems better than the Narloy-Z alloy. The failure mode of the thrust chamber ligament is instability, but the Narloy-Z alloy has better resistance against fatigue and creep failure. The following results may also be for the same reason.

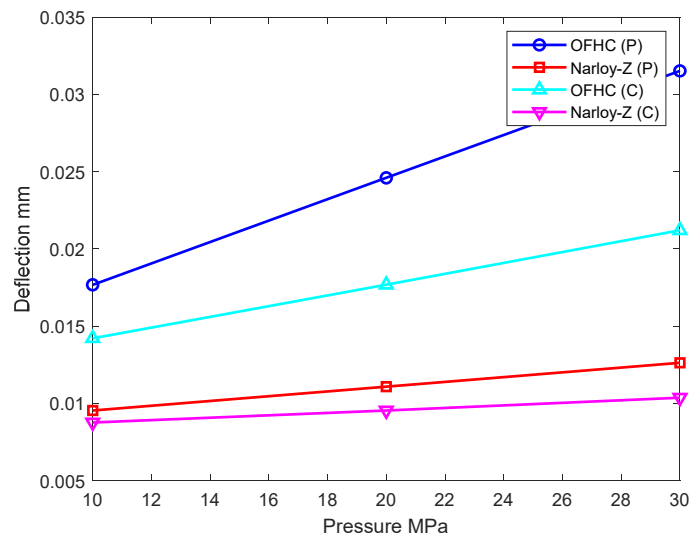


**Figure 6.** Pressure difference and deflection.

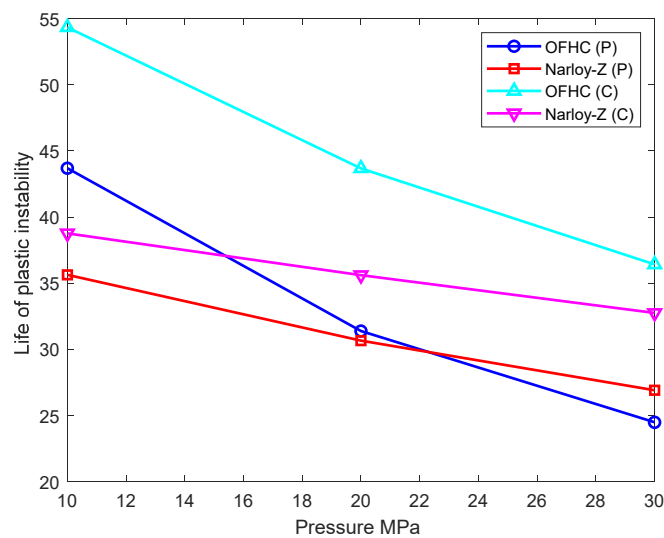


**Figure 7.** Pressure difference and life of instability.



#### 4.2. Temperature Difference

The temperature difference between the ligament also influences the deflection per cycle and the life of instability. For regeneratively cooled thrust chamber ligament, changes in the temperature difference influence the total deflection and instability life. Usually, the thickness variation of the inner wall affects the heat transfer coefficient of the thrust chamber wall, and then the temperature difference of the inner wall changes. According to the heat transfer calculation results mentioned above, the temperature difference between the inner wall at the throat section is 135.41 K (243.73 °F). For different inner wall materials, the temperature difference is not the same, so the change interval of the inner wall temperature difference range is taken 100–500 K for analysis.

With the increase of the inner wall temperature difference, the total deflection decreases first and then increases because of the quadratic function of  $\Delta T$ . Compared with Narloy-Z alloy, the variation in the total deflection of OFHC copper is more obvious in Figure 8. From the results, it can be concluded that under the pressure difference of 18 MPa, the maximum instability life of OFHC and Narloy-Z thrust chamber is about 38 lifetimes in Figure 9. The results have the same tendency for the two beam models for the life of instability because the deflection  $\delta_3$  is quite small in the calculation. Therefore, controlling the temperature difference of the inner wall ligament is an important measure to prolong the life of the thrust chamber of reusable liquid rocket engines.

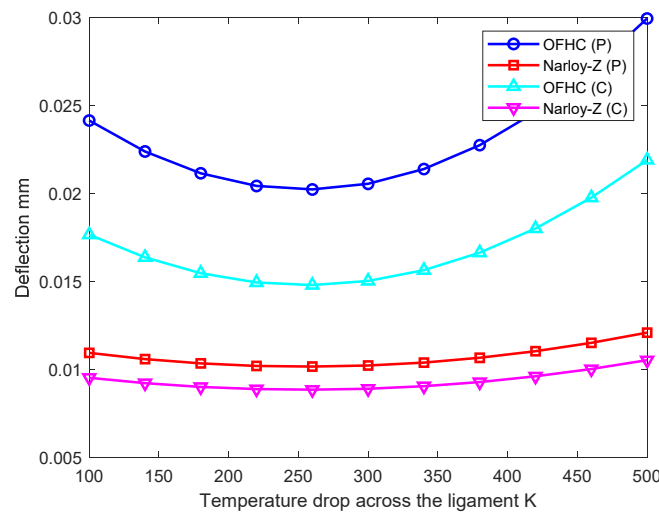


Figure 8. Temperature difference and deflection.

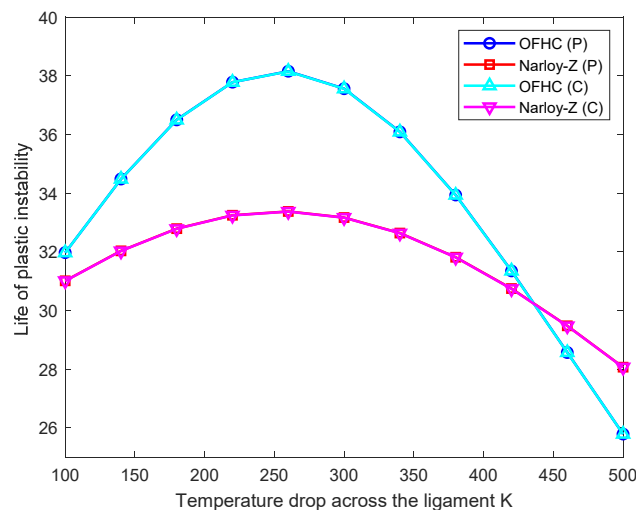


Figure 9. Temperature difference and life of instability.

### 4.3. Thickness of Ligament

The inner wall suffers from high pressure and temperature difference during engine combustion. The thickness of the inner wall ligament is generally in the order of millimeters, which is extremely vulnerable to damage during each firing cycle. The thickness increase in the ligament intensifies the structural strength, but the temperature difference of the ligament increases due to heat transfer coefficient variation. During the analysis of instability life, the temperature difference caused by the variation of thickness is ignored.

Increasing the inner wall thickness significantly reduces the total deflection and increases the instability life in Figure 10. The life of OFHC in the Porowski beam is higher than that of Narloy-Z, and the life of Narloy-Z is higher in the creep-modified model is shown in Figure 11. The reason is that the change in the inner wall thickness has a great influence on the total deflection, and when other conditions remain invariant, the life of instability is inverse to the total deflection.

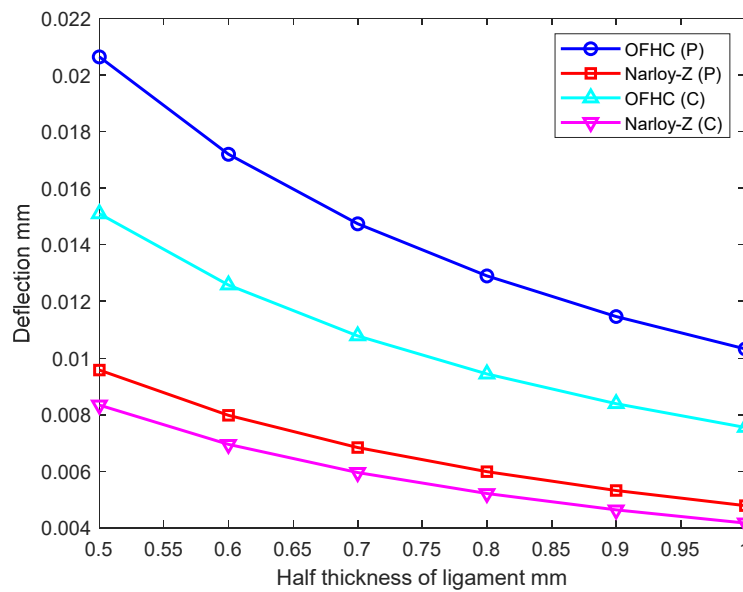


Figure 10. Thickness of ligament and deflection.

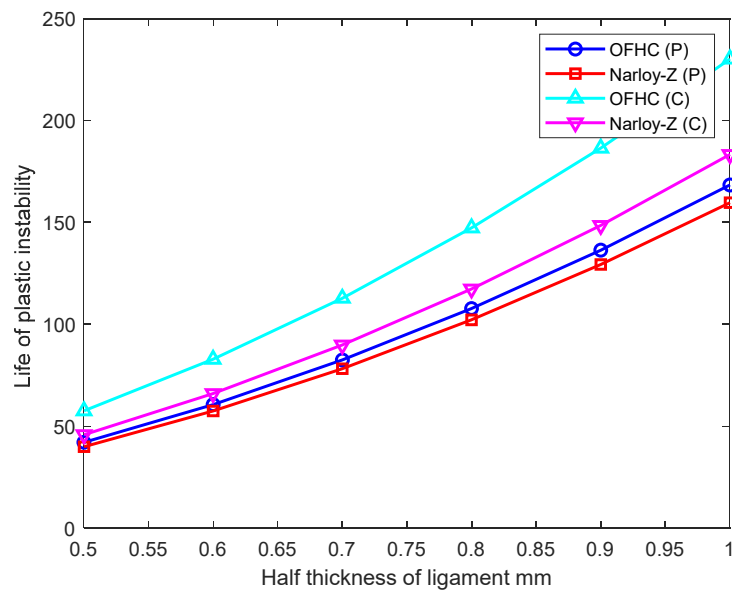


Figure 11. Thickness of ligament and life of instability.

#### 4.4. Width of Coolant Channel and Rib

The width of the coolant channel affects the life of the inner wall ligament in the thrust chamber, and the width of the coolant channel is usually in the order of millimeters. In the analysis of the total deflection and instability life of the inner wall, the interval of width is from 1 mm to 4 mm. The width of the rib only influences the instability life of the thrust chamber wall according to the Porowski beam model and the creep-modified model.

The total deflection increases with the width of the coolant channel while the instability life of the inner wall decreases. In the creep-modified model, the total deflection of the inner wall increases significantly when the groove width is 3.5 mm in Figure 12, so the life of instability decreases rapidly in Figure 13. The cause of this increase is the coolant width power in  $\delta_3$ . With the increase of rib width, the instability life of the thrust chamber wall shows a tendency to decrease in Figure 14, and the same reason could explain the similar results of the two models in Figure 9. However, Porowski beam models are unable to analyze the relationship between rib width and deflection.

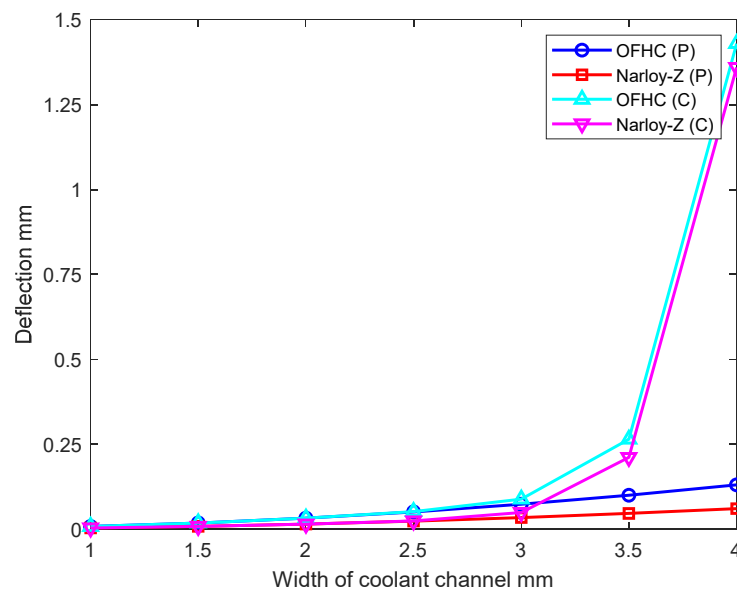


Figure 12. Width of coolant channel and deflection.

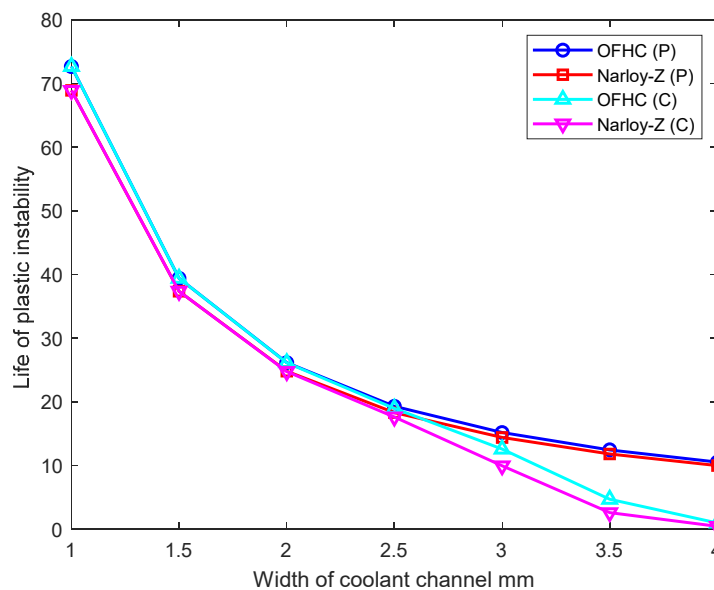
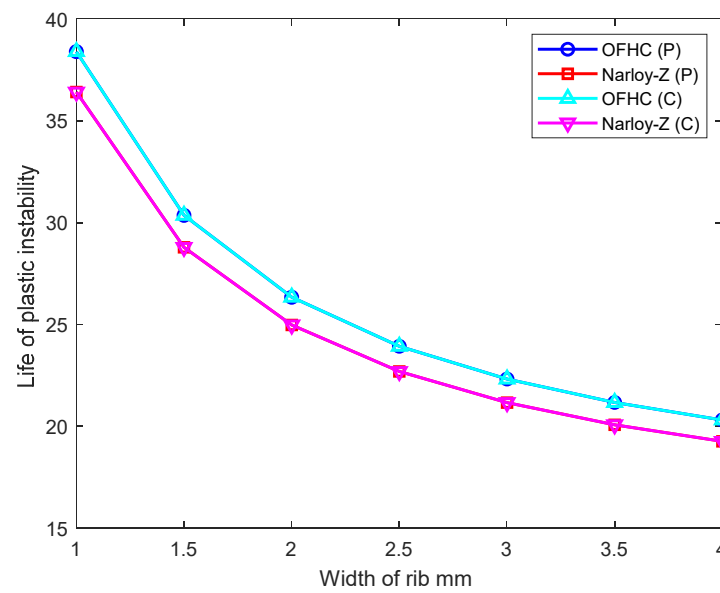


Figure 13. Width of coolant channel and life of instability.



**Figure 14.** Width of rib and life of instability.

#### 4.5. Rib Filling Ratio

The rib filling ratio, also called the width ratio of the rib and coolant channel which, is defined as the width of the coolant channel divided by the width of the rib,  $\eta = l/w$ . The rib filling ratio was referenced in many articles; however, no quantified analyses were performed. In this study, the life of instability,  $t_{\min}$ , and  $t_{\max}$  of the inner wall ligament were analyzed when the rib filling ratio changed. The asymptotic lines were deduced simply with the following equations.

$$t_{\min} = 2H - \frac{Nw\delta}{l+w} = 2H - \frac{N\delta}{\eta+1} \quad (22)$$

$$\lim_{\eta \rightarrow \infty} t_{\min} = 2H \quad (23)$$

$$t_{\max} = 2H + \frac{Nwl\delta}{(l+w)^2} = 2H + \frac{N\delta}{\eta+2+\frac{1}{\eta}} \quad (24)$$

$$\lim_{\eta \rightarrow \infty} t_{\max} = 2H \quad (25)$$

$$\eta + \frac{1}{\eta} \geq 2\sqrt{\frac{1}{\eta} \cdot \eta} \Rightarrow t_{\max} \leq 2H + \frac{N\delta}{4} \quad (26)$$

From Equation (26), we know that only when  $\eta = 1$ ,  $l = w$  which means the width of the rib and coolant channel are the same, then the maximum thickness of the ligament is achieved at  $t_{\max} = 2H + \frac{N\delta}{4}$ .

With the increase of the ratio of the rib and coolant channel, the effective strain range decreases in Figure 15. The reason is that the ratio of  $t_{\max}$  and  $t_{\min}$  value is contained in the effect strain range according to Equations (13) and (14). Therefore, it can be seen that the ratio of  $t_{\max}$  and  $t_{\min}$  value has the same reduction with the effective strain range when the rib width ratio is increasing. Figures 16–18, the maximum ligament thickness of Narloy-Z is lower than OFHC, and the minimum ligament thickness is higher than OFHC under different cycles. This suggests that Narloy-Z has a slower rate of deformation than OFHC. Hence, Narloy-Z is more suitable for thrusting inner walls.

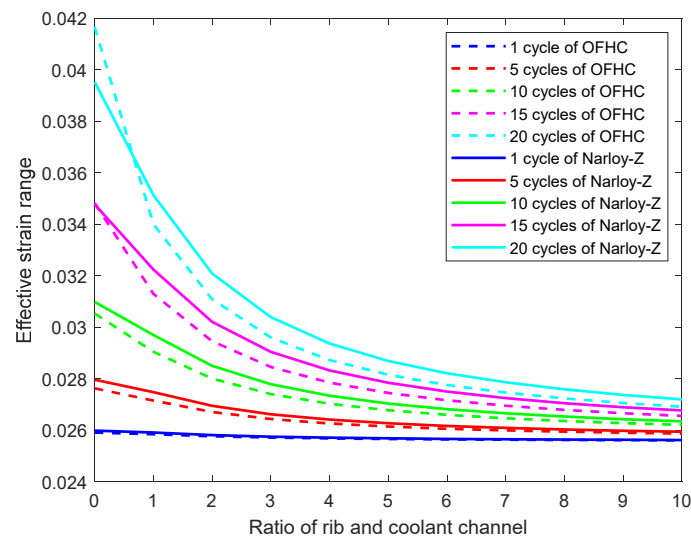


Figure 15. Ratio of rib and coolant channel with effective strain range.

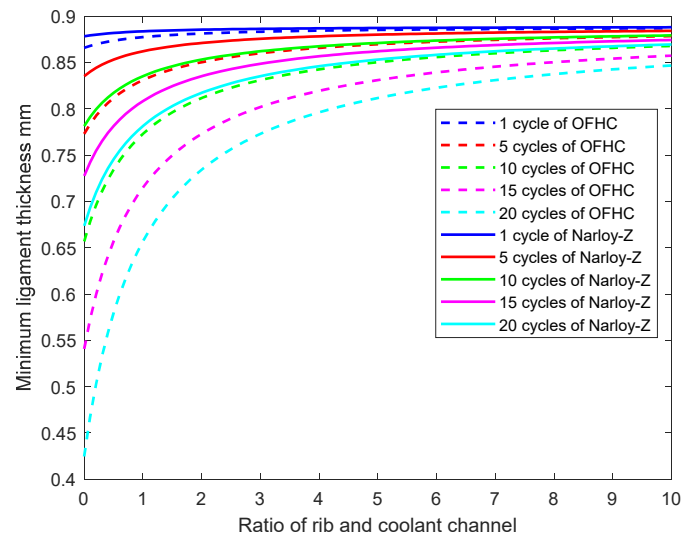


Figure 16. Ratio of rib and coolant channel with minimum ligament thickness.

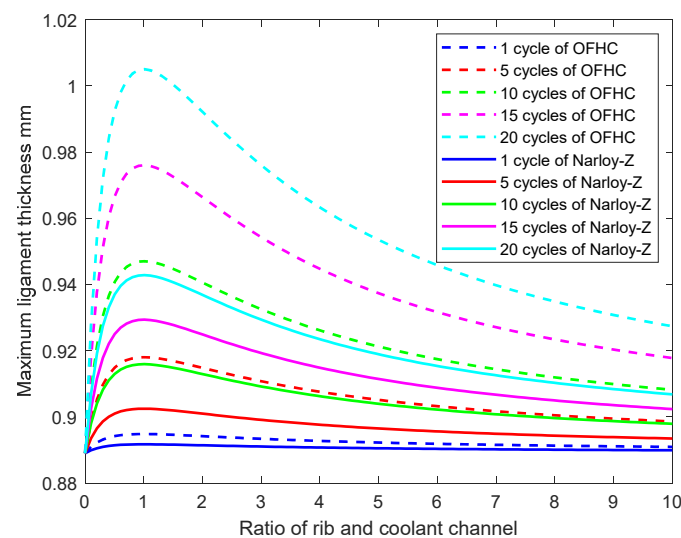
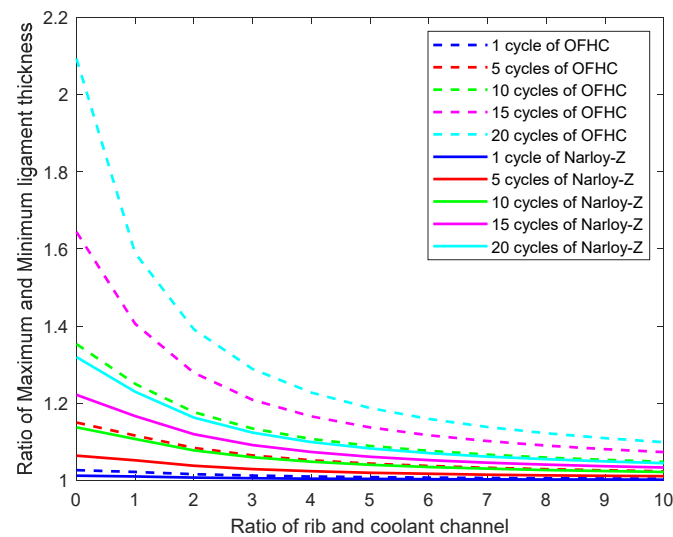


Figure 17. Ratio of rib and coolant channel with maximum ligament thickness.



**Figure 18.** Ratio of rib and coolant channel with the ratio of maximum and minimum ligament thickness.

## 5. Conclusions

With the development of reusable liquid rocket engines, life prediction is receiving increasing attention in aerospace. This research performed a quantitative analysis of life prediction based on the Porowski beam model and the creep-modified model for a LOX/Kerosene rocket engine thrust chamber.

From the life analysis, we can draw a conclusion that the pressure and temperature difference, structural parameters and material parameters have a significant impact on the deflection per cycle and life of instability. With the increasing pressure difference, the deflection increases as well, and the life of instability decreases. The temperature difference between deflection and life seems to have a relationship with the quadratic function. During the design of reusable liquid rocket engine thrust chambers, pressure and temperature difference have to be strictly constrained to extend the lifetime. The life of instability goes up when the thickness of the inner wall ligament grows. When the width of the rib and coolant channel increase, the life of instability reduces clearly. The rib filling ratio plays an important role in ligament thinning; the asymptotic line of  $t_{\max}$ ,  $t_{\min}$  and effective strain range appears when the rib filling ratio is augmented. This situation of widths of the same value in ribs and coolant channels should be avoided in structural design and manufacturing. From the analysis, Narloy-Z alloy is better than OFHC copper for thrust chamber inner wall material because of the lower deformation rate.

Life analysis conducted in this research offered an appropriate reference for the design and manufacturing of reusable liquid rocket engine thrust chambers.

**Author Contributions:** Conceptualization, Y.Q. and Y.C.; Methodology, Y.C.; Software, Y.Z.; Validation, Y.Z. and Y.C.; Formal analysis, Y.Q.; Investigation, Y.Q.; Resources, Y.C.; Data curation, Y.Q.; Writing—original draft preparation, Y.Q. and Y.C.; Writing—review and editing, Y.Q.; Visualization, Y.C.; Supervision, Y.C. and Y.Z.; project administration, Y.C. All authors have read and agreed to the published version of the manuscript.

**Funding:** This research received no external funding.

**Institutional Review Board Statement:** Not applicable.

**Informed Consent Statement:** Not applicable.

**Data Availability Statement:** Data is contained within the article.

**Conflicts of Interest:** The authors declare no conflict of interest.

## References

1. Kasper, K.J. Thrust Chamber Life Prediction. NASA. 1985. Available online: <https://ntrs.nasa.gov/citations/19850018554> (accessed on 1 October 2022).
2. Asraff, A.K.; Sunsil, K. Stress analysis & life prediction of a cryogenic rocket engine thrust chamber considering low cycle fatigue, creep and thermal ratchetting. *Trans. Indian Inst. Met.* **2010**, *63*, 601–606.
3. Asraff, A.K.; Babu, S.S.; Babu, A.; Eapen, R. Application of Chaboche Model in Rocket Thrust Chamber Analysis. *J. Inst. Eng. India Ser. C* **2017**, *98*, 227–233. [[CrossRef](#)]
4. Schwarz, W.; Schwub, S. Life prediction of thermally highly loaded components: Modelling the damage process of a rocket combustion chamber hot wall. *CEAS Space J.* **2011**, *1*, 83–97. [[CrossRef](#)]
5. Tong, J.; Hou, C.T.; Jia, L. The analysis of the fracture problem of the inner wall of thrust chamber causing by muster and ablation. *Struct. Environ. Eng.* **2013**, *40*, 29–35.
6. Cheng, C.; Wang, Y.B.; Liu, Y.; Liu, D.W.; Lu, X.Y. Thermal-structural response and low-cycle fatigue damage of channel wall nozzle. *Chin. J. Aeronaut.* **2013**, *26*, 1449–1458. [[CrossRef](#)]
7. Zhang, S.; Jin, P.; Cai, G.B. Structural reliability simulation and parameter sensitivity analysis of cooling channel for thrust chamber. *J. Aerosp. Power* **2018**, *33*, 2651–2659.
8. Ferraiuolo, M.; Riccio, A. Study of the Effects of Materials Selection for the Closeout Structure on the Service Life of a Liquid Rocket Engine Thrust Chamber. *J. Mater. Eng. Perform.* **2019**, *28*, 3186–3195. [[CrossRef](#)]
9. Ferraiuolo, M.; Perrella, M.; Giannella, V.; Citarella, V. Thermal–Mechanical FEM Analyses of a Liquid Rocket Engines Thrust Chamber. *Appl. Sci.* **2022**, *12*, 3443. [[CrossRef](#)]
10. Ferraiuolo, M.; Leo, M.; Citarella, R. On the Adoption of Global/Local Approaches for the Thermomechanical Analysis and Design of Liquid Rocket Engines. *Appl. Sci.* **2020**, *10*, 7664. [[CrossRef](#)]
11. Citarella, R.; Ferraiuolo, M.; Perrella, M.; Giannella, V. Thermostructural Numerical Analysis of the Thrust Chamber of a Liquid Propellant Rocket Engine. *Materials* **2022**, *15*, 5427. [[CrossRef](#)] [[PubMed](#)]
12. Liu, D.; Sun, B.; Wang, T.P.; Song, J.W.; Zhang, J.W. Thermo-structural analysis of regenerative cooling thrust chamber cylinder segment based on experimental data. *Chin. J. Aeronaut.* **2020**, *33*, 102–115. [[CrossRef](#)]
13. Daniel, T.B. RLV Thrust Cell Liner Coating Analysis and Design Considerations. In Proceedings of the 44th AIAA/ASME/ASCE/AHS Structures, Structural Dynamics, and Materials Conference, Norfolk, VA, USA, 7–10 April 2003.
14. Ray, A.; Dai, X.W. Damage-Mitigating Control of a Reusable Rocket Engine for High Performance and Extended Life. NASA CR-4640; 1995. Available online: <https://ntrs.nasa.gov/citations/19950016778> (accessed on 1 October 2022).
15. Ray, A.; Dai, X.W. Damage-Mitigating Control of a Reusable Rocket Engine: Part I—Life Prediction of the Main Thrust Chamber Wall. *J. Dyn. Syst. Meas. Control.* **1996**, *11*, 401–408.
16. Porowski, J.S.; Badlani, M. Development of a Simplified Procedure for Thrust Chamber Life Prediction. NASA CR-165585; 1981. Available online: <https://ntrs.nasa.gov/citations/19820013379> (accessed on 1 October 2022).
17. Porowski, J.S.; Badlani, M. Simplified Design and Life Prediction of Rocket Thrust Chambers. *Am. Inst. Aeronaut. Astronaut.* **1985**, *2*, 182–187. [[CrossRef](#)]
18. Porowski, J.S.; Badlani, M. Development of a Simplified Procedure for Rocket Engine Thrust Chamber Life Prediction with Creep. NASA CR-168261; 1984. Available online: <https://ntrs.nasa.gov/citations/19840011404> (accessed on 1 October 2022).
19. Niino, M.; Kumakawa, A. Evaluation of Cold Isostatic Pressing of High-Pressure Thrust Chamber Closeout. *J. Propuls.* **1986**, *2*, 25–30. [[CrossRef](#)]
20. Sung, I.K.; Anderson, W. A Subscale-Based Rocket Combustor Life Prediction Methodology. In Proceedings of the 41st AIAA/ASME/SAE/ASEE Joint Propulsion Conference and Exhibit, Tucson, AZ, USA, 10–13 July 2005.
21. Chen, T.; Yang, J.H.; Jin, P.; Sun, B.; Cai, G.B. Design and Analysis for Reusable Liquid Rocket Engine Chamber. In Proceedings of the 49th AIAA/ASME/SAE/ASEE Joint Propulsion Conference, San Jose, CA, USA, 14–17 July 2013.
22. Marco, P. An Algebraic Model for Structural and Life Analysis of Regeneratively-Cooled Thrust Chambers. *J. Propuls. Power* **2020**, *36*, 191–201. [[CrossRef](#)]
23. Marco, P.; Barbara, B.; Francesco, N. Cooling Channel Analysis of a LOX/LCH4 Rocket Engine Demonstrator. In Proceedings of the 50th AIAA/ASME/SAE/ASEE Joint Propulsion Conference, Cleveland, OH, USA, 28–30 July 2014.
24. Hannum, N.P.; Kasper, H.J.; Pavli, A.J. Experimental and theoretical investigation of fatigue life in reusable rocket thrust chambers. In Proceedings of the AIAA/ASME 12th Propulsion Conference, Palo Alto, CA, USA, 26–29 July 1976.
25. Quentmeyer, R.J. Experimental fatigue life investigation of cylindrical thrust chambers. In Proceedings of the AIAA/ASME 13th Propulsion Conference, Orlando, FL, USA, 11–13 July 1977.
26. John, J.E.; Ronald, F.Z. Thrust Chamber Life Prediction Volume I—Mechanical and Physical Properties of High Performance Rocket Nozzle Materials. NASA CR-134806; 1975. Available online: <https://ntrs.nasa.gov/citations/19750021165> (accessed on 1 October 2022).
27. Qi, Y.J.; Cheng, Y.Q.; Zhang, Z.Z. Life prediction and damage calculation of reusable liquid rocket engine thrust chamber. In Proceedings of the 3rd International Symposium on Robotics & Intelligent Manufacturing Technology (ISRIMT), Changzhou, China, 24–26 September 2021.